

Estimation of evapotranspiration rate in the Sahelian region of Nigeria using Generalized Regression Neural Network and Feed Forward Neural Network

Habeeb Ajibola Yusuf^{1,2}, Nelson Agbaje², Idowu Ezekiel Olorunfemi^{2*}

(1. Department of Forest Resources Management, University of British Columbia, Canada ;

2. Department of Agricultural and Environmental Engineering, Federal University of Technology, Akure, Nigeria)

Abstract: Artificial Neural Network (ANN) was employed by researchers in obtaining accurate estimates of evapotranspiration rate. Generalized Regression Neural Network (GRNN) and Feed Forward, Back Propagation Neural Network (FFBP NN) were used to estimate evapotranspiration rate in Kano State, Northern Nigeria to ascertain its modelling accuracy under less input parameters. A 25-year monthly-time step of climatological data was collected from International Institute of Tropical Agriculture (IITA) station. The data were grouped into 12 different input combination with training and validation sets. Based on performance ranking of input combinations used in different neural networks, the solar radiation (GRNNSr) with a Root Mean Square Error (RMSE) of 1.982 ranked lowest while the temperature and wind speed combination input (GRNNTW) ranked highest with a Root Mean Square Error (RMSE) of 0.7777. Observations indicated similar input combinations ranking with the two-layered Feed Forward Neural Network (FFNN) (with 10 hidden neurons). The input combination of temperature, wind speed and solar radiation had the best performance under the Feed Forward Back Propagation Neural Network (FFBP NN) with RMSE as low as 0.6333. This is contrast to the input combination of solar radiation and humidity, which had the lowest performance under the FFBP NN with RMSE of 1.3512. The input combination of temperature and wind speed is the most preferred input combination, having less data input and higher performance. Observations indicated that wind speed provides the best estimate of evapotranspiration in the region than all other lone inputs. Overall, FFBN showed the highest potential in estimating evapotranspiration in the Sahelian region of Nigeria under limited climatological input parameters.

Keywords: Evapotranspiration, Artificial Neural Network, Generalized Neural Network, Feed- Forward Neural Network.

Citation: Yusuf, H. A., N. Agbaje and I. E. Olorunfemi. 2020. Estimation of evapotranspiration rate in the Sahelian region of Nigeria using Generalized Regression Neural Network and Feed Forward Neural Network. *Agricultural Engineering International: CIGR Journal*, 22(4): 31-39.

1 Introduction

Received date: 2019-07-20 **Accepted date:** 2019-11-03

***Corresponding author: I. E. Olorunfemi**, Ph.D, Department of Agricultural and Environmental Engineering, Federal University of Technology, Akure, Nigeria, +2347037986945, olorunfemiidowu@gmail.com.

Agriculture has the highest percentage of water withdrawals accounting for about 70% of the total global water withdrawals from fresh water sources. Water for irrigation is rapidly increasing and expected to increase by 10% at 3000 km³ year⁻¹ by 2050 for increased crop productivity to avoid food insecurity for the projected 6.9 billion humans living on planet earth (FAO, 2011). The estimation of evapotranspiration (*ET*) is very important and crucial for the determination of crop consumptive use in the

design of irrigation systems and water management structures for farms. In the past, *ET* has been employed in the modeling and simulation of stream flow, hence the need for good reference evapotranspiration estimators. The most widely used methods of estimating *ET* are through the use of evaporation pan, soil water depletion, water balance, lysimeters, energy balance and mass transfer, field experimental plots and from climatological data using empirical formulas (Micheal, 1978; Ward and Trimble, 2003). Empirical formula has the advantage of speed and accuracy depending on the model suitability, such estimators includes Blaney–criddle model, Szast, Kharuffa, Thornthwaite, Hagreaves Samani, Makkink, Turc, Priestly Taylor etc. Ilesanmi et al. (2014) used a 29-year data from International Institute of Tropical Agriculture (IITA) to estimate *ET_o* with various *ET* models, there were degrees of variation across all models, but the Blaney-Morin Nigeria (BMN) model proved to be the best model for evaluating *ET_o* indicating its accuracy and consistency in the estimation of *ET_o* in Nigeria.

Artificial Neural Network (ANN) model is essentially a black box that relates known inputs to output for a well-defined training set, to model complex non – linear process or functions, by creating a connection known as weights between the neurons in the Network system which can be achieved through supervised or non-supervised learning process (Kriesel, 2007; Landeras et al., 2008; Traore et al., 2008; Heddam et al., 2013). The use of ANN in the field of hydrological research, rainfall estimation, flow forecasting, rainfall – runoff process, river sediment flux modelling, evapotranspiration process modelling has also been reported (Deo and Şahin, 2015; Hosseini and Mahjouri, 2016; Guven and Kisi, 2013; Nourani, 2016; Prasad et al., 2017). Generalized Regression Neural Network (GRNN) and Feed Forward Neural Network (FFNN) have been employed in many areas for optimization hydrological models (Kişi, 2006; Tuan Resdi and Lee, 2014). Feng et al. (2017) modelled reference *ET* using extreme learning machine and generalized regression neural network using only temperature data. However, no reported work has been

carried out on the use of ANN in estimating *ET* in the Sahel region of Nigeria. This research examines the potential of Generalized Regression and Feed Forward – Back Propagation Neural Network in estimating *ET* in the Sahelian region of Nigeria (Kano) with an intent of finding the best possible meteorological input combination.

2 Materials and methods

2.1 Study area

Kano is located in the north – western part of Nigeria, within the Sahelian region of Sudan with annual rainfall between 800 to 1100 mm across the state. It satisfies the koppen classification of *A_w* (winter dry season) it has latitude between 10°30'N to 12°38'N and longitudes spanning between 7°45'E to 9°29'E with an average altitude of 486 m (Nwagbara, 2015; Maina et al., 2012). It records an annual temperature of about 26°C, with maximum upper threshold temperature of 38°C and minimum lower threshold temperature 21°C (Gbode et al., 2015).

2.2 GRNN architecture

The GRNN was first developed by Donald F. Specht in the year 1991. He defined the memory based network as a “one-pass learning algorithm with a highly parallel structure” and given a sparse data the algorithm can provide a smooth transition from one observed value to another (Specht, 1991). The GRNN Architecture has four layers, which are the input layer, hidden layer: pattern and summation layer (S-summation layer, D-summation layer) and the output layer. The pattern neuron consists of units that have stored patterns which serve as training patterns to give an output that is a measure of the Euclidean distance of the input pattern and the stored pattern. The summation neuron; S- summation which sums the weighted outputs from pattern neuron, and the D-summation which computes the output with unity weight. A parameter known as the spread or width factor (σ) an assumed value that defines the extent of generalization the network can take. From the S–summation, neuron connects each to the pattern neuron, the output layer thus divides each S –summation neurons by the D-summation neurons to obtain the vector output (Singh

and Deo, 2006). The output vector is given as:

$$Y_i = \frac{\sum_{i=1}^n y_i e^{-D(x, x_i)}}{\sum_{i=1}^n e^{-D(x, x_i)}} \quad (1)$$

$$D(x, x_i) = \sum_{k=1}^q \left(\frac{x_k - x_{ik}}{\sigma} \right) \quad (2)$$

Where; Y_i = predicted value to an unknown input vector x , y_i = target output, D = distance to training sample from the prediction data, x_i = input vector, σ = spread, n indicates the number of training patterns, p indicates the number of elements of an input vector or total number of input nodes, The x_k and x_{ik} represent the k th element of x and x_i , respectively. The pros of the GRNN over the other ANN architecture are that it can work with sparse training data set as shown in Figure 1. Its approach allows the network to converge to the optimal regression surface faster due to its fast learning. There is also no sensitivity to random initial weights in the input layer, unlike the back propagation network which requires iterative training. The GRNN is a one pass learning algorithm. It has also been reported that there is no problem of local minima. (Hannan et al., 2010; Kişi, 2006; Sengupta et al., 2013; Traore et al., 2008; Specht, 1991).

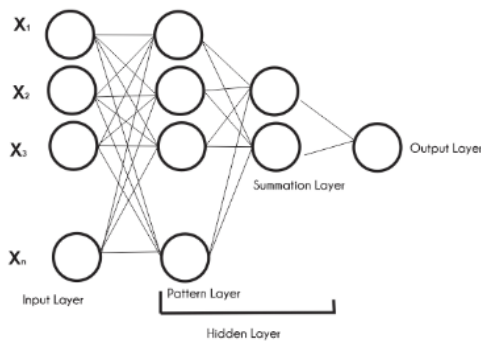


Figure 1 GRNN architecture

2.3 FFBP architecture

The Feed Forward network is a simple neural network with information from the input through the hidden node to the output, going in a unidirectional path. The network architecture is a sigmoid transfer function in the hidden – layer and the linear transfer function in the output layer as configured on the Matlab R2013a ‘nnfit’ GUI using the back propagation Levenberg – Marquardt training algorithm

as shown below.

$$x_{ij} = x_i - (H + \mu)^{-1}_K g_K \quad (3)$$

Where; x_i = biases vector, H = hessian matrix of the performance index at x_i , g_k = gradient at x_i , μ is a scalar algorithm constant, j is the jacobian matrix that contain first derivatives of the network errors with respect to weights and biases. The architecture of the FFBP is shown below.

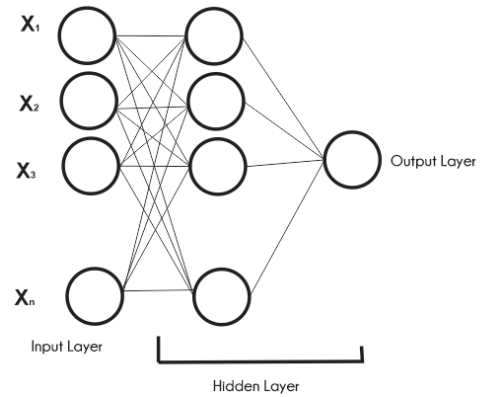


Figure 2 Feed Forward, Back Propagation Neural Network architecture

2.4 Penman-Monteith (FAO’56)

The standard reference model for the estimation of ET is the FAO’56 Penman-Monteith Model (Antonopoulos and Antonopoulos, 2017). The typical model is shown below:

$$ET_o = \frac{0.408\Delta(R_n - G) + \gamma \frac{C_n}{T + 273} u_2 (e_s - e_a)}{[\Delta + \gamma(1 + C_d U_2)]} \quad (4)$$

Where ET_o is the daily reference crop ET (mm d^{-1}), C_n and C_d is the numerical constant that changes with reference surfaces (mms³Mg⁻¹d⁻¹), R_n is the net radiation (MJ $m^{-2} d^{-1}$), u_2 is the mean wind speed at 2 m above soil surface (ms⁻¹), T is the mean air temperature(°C), G is the soil heat flux density at the soil surface (MJ $m^{-2} d^{-1}$), e_a is the saturation vapour pressure (kPa), e_s is the actual vapour pressure (kPa), Δ is the slope of the saturation vapour pressure temperature curve (kPa °C⁻¹), γ is the psychrometric constant (kPa °C⁻¹).

2.4.1 Data

The input data set is sourced from a 25-year monthly - time step (1993-2017) data of meteorological data collected

from the IITA station in Kano, which includes: temperature (Min. and Max.) in °C, relative humidity (Min. and Max.) in %, sunshine hours, rainfall intensity in mm, solar radiation in MJ m⁻² d⁻¹, pan evaporation in mm day⁻¹, and wind speed in m s⁻¹. Table 1 indicates the various input combinations used for investigation in this research. Standardization is achieved by making the mean 0 and the standard deviation 1. MATLAB uses the 'mapstd' function to achieve this.

S/N	Combination	No of Variables
1	T, H, S	3
2	T, W, S	3
3	T	1
4	S	1
5	T, H, W, S	4
6	T, S	2
7	T, W	2
8	S, W	2
9	S, H	2
10	T, W, H	3
11	S, W, H	3
12	W	1

Note: T= temperature, H= humidity, S= solar radiation, W= wind speed.

3 Results and discussions

The Penman Monteith reference *ET_o* was computed on an excel worksheet and the results of each month's estimated *ET_o* were compared with the predicted *ET_o* from the GRNN Network, trained with 70% of the combination input data and tested with 30% of the same data using the Matlab R2013a, Version 8.1.0.604. The predicted *ET_o*'s data set obtained was used to compute the R, R-squared, Mean Square Error (MSE), Root Mean Square Error (RMSE). The optimized spread between 0.01 and 1 required for the best regression fit was obtained after an iteration process to obtain the best regression fit and least error in the calibration process. The ranking of each input combination was considered on the scale of 1-12 for the best statistical indicator performance. Table 2 presents the statistical performance of different input combination using the FFNN.

Table 2 Statistical performance of the various input combination using the GRNN.

		GRNN											
		THS	TWS	T	S	ALL	TS	TW	SW	SH	TWH	SWH	W
R	Val.	0.5465	0.7494	0.4169	0.3603	0.7606	0.5446	0.7925	0.5801	0.3973	0.7458	0.6855	0.6457
	Cal.	0.8158	0.9251	0.5099	0.3550	0.9571	0.664	0.8983	0.7449	0.4425	0.9188	0.8432	0.7019
R²	Val.	0.2987	0.5616	0.1738	0.1298	0.5786	0.2966	0.6281	0.3399	0.1579	0.5563	0.4699	0.4170
	Cal.	0.6665	0.8558	0.2598	0.1122	0.9160	0.4441	0.8071	0.5549	0.1958	0.8441	0.7110	0.4927
MSE	Val.	1.1483	0.712	1.3505	1.4356	0.7029	1.1761	0.6048	1.1051	1.3856	0.7368	0.9144	1.0499
	Cal.	0.8402	0.4001	1.6283	1.8207	0.2737	1.3161	0.4762	1.0027	1.6788	0.4182	0.7169	1.1277
RMSE	Val.	1.0716	0.8438	1.1162	1.1982	0.8384	1.0845	0.7777	1.0512	1.1771	0.8584	0.9563	1.0246
	Cal.	0.9166	0.6325	1.2703	1.3493	0.5231	1.1472	0.6901	1.0014	1.2957	0.6467	0.8467	1.069
σ													
(Spread)		0.5	0.39	0.77	0.95	0.42	0.81	0.23	0.39	0.71	0.35	0.25	0.29
No.of Var.		3	3	1	1	4	2	2	2	2	3	3	1
Avg. Rank		8	3	9	11	2	10	1	7	12	4	5	6

The scatter plot of the various input Combination used for training and validating the GRNN is shown from Figure 3 through to Figure 14. A two - layered Feed Forward Neural Network, with Levenberg – Marquadt back propagation training algorithm, using 10 hidden neurons in the hidden layer with sigmoid transfer function was used. The dataset was randomly divided into 70% training, 10%

validation and 20% testing, the MATLAB R2013 nfitool were used to train the Network, the R and MSE results obtained are chosen after a number of epochs and retrains, after which the seemingly best R and MSE are selected. Table 3 shows the statistical indicators as well as the average ranking of the indicators of the FFNN Neural Network for the various input combinations.

Table 3 Statistical performance of the various input combinations using the FFNN.

	FFNN											
	THS	TWS	T	S	ALL	TS	TW	SW	SH	TWH	SWH	W
R	0.6029	0.9167	0.5163	0.4832	0.9091	0.6029	0.8585	0.6995	0.4662	0.8925	0.7840	0.7111

R²	0.3635	0.8301	0.2665	0.2334	0.8263	0.3635	0.7370	0.4893	0.2177	0.7965	0.6146	0.5056
MSE	0.8670	0.4011	1.4865	1.2730	0.4238	1.5812	0.4715	1.0794	1.8259	0.4842	0.8356	0.8446
RMSE	0.9311	0.6333	1.2192	1.1283	0.6509	1.2574	0.6866	1.0389	1.3512	0.6958	0.9141	0.9190
No.	10	10	10	10	10	10	10	10	10	10	10	10
Neuron												
No.of Var.	3	3	1	1	4	2	2	2	2	3	3	1
Avg.	8	1	9	10	2	11	3	7	12	4	5	6
Rank												

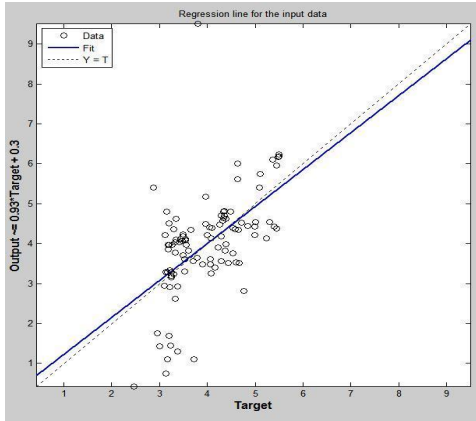


Figure 3 Scatter plot of the GNNTHS input combination

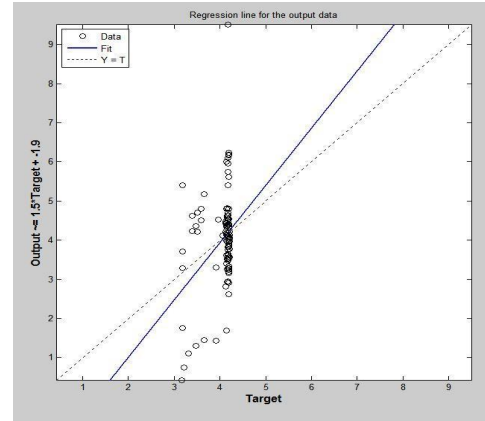


Figure 6 Scatter plot of the GNNS input combination

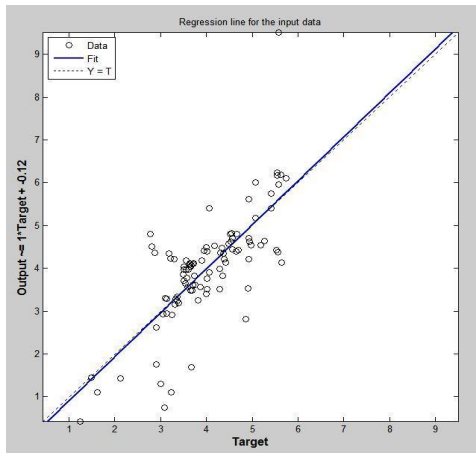


Figure 4 Scatter plot of the GNNTWS input combination

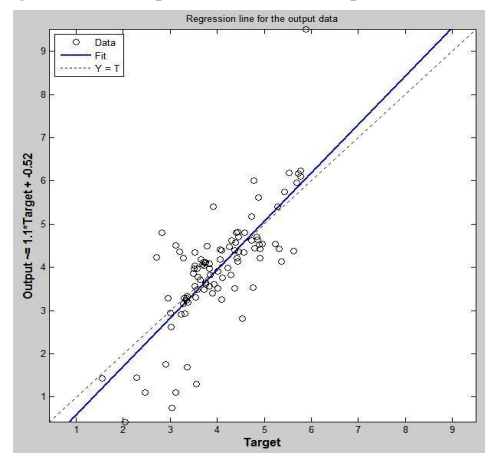


Figure 7 Scatter plot of the GNNALL input combination

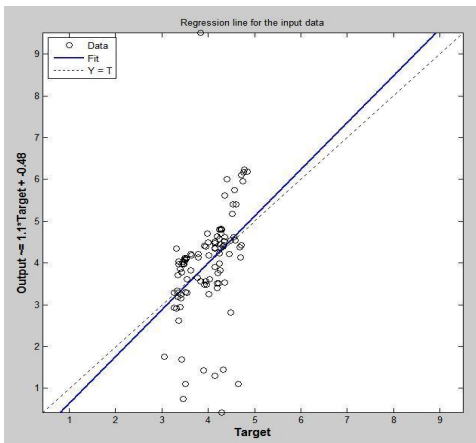


Figure 5 Scatter plot of the GNNT input combination

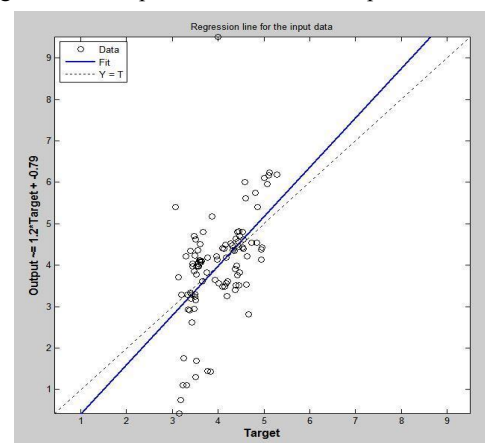


Figure 8 Scatter plot of the GNNTS input combination

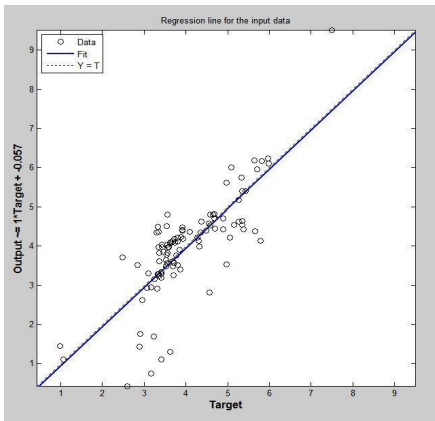


Figure 9 Scatter plot of the GNNTW input combination

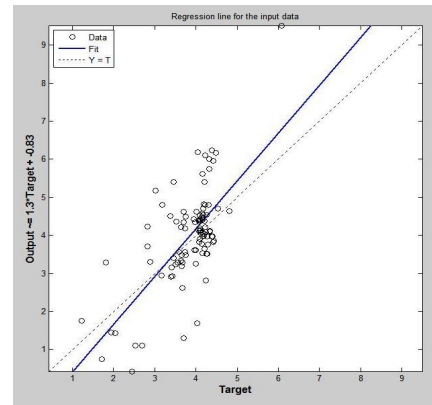


Figure 13 Scatter plot of the GNNSWH input combination

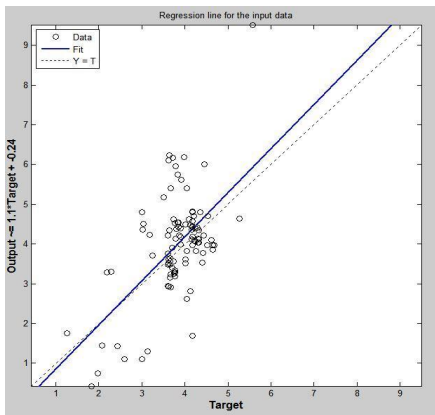


Figure 10 Scatter plot of the GNNSW input combination

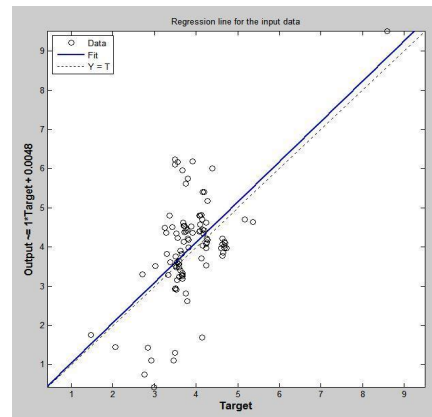


Figure 14 Scatter plot of the GNNW input combination

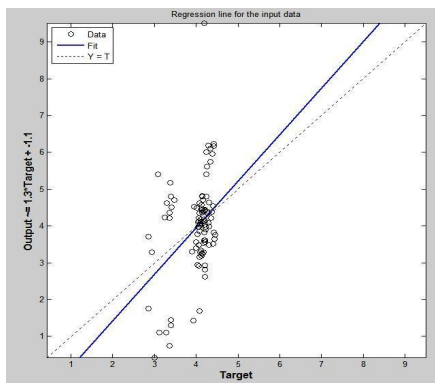


Figure 11 Scatter plot of the GNNSH input combination

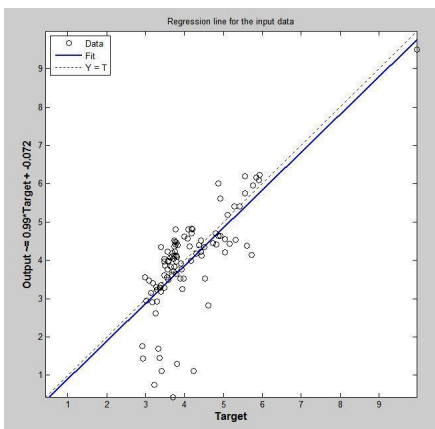
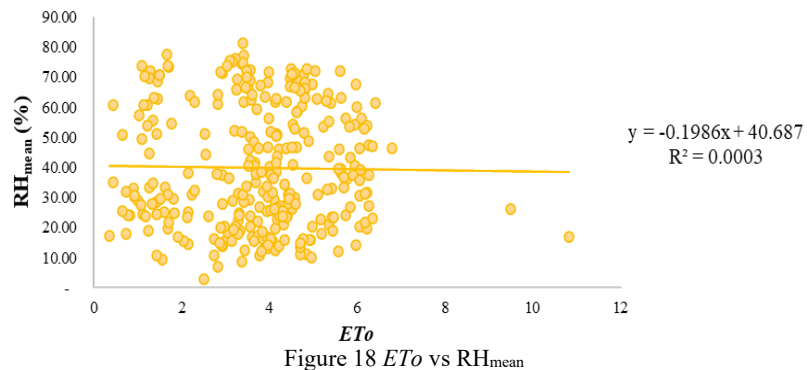
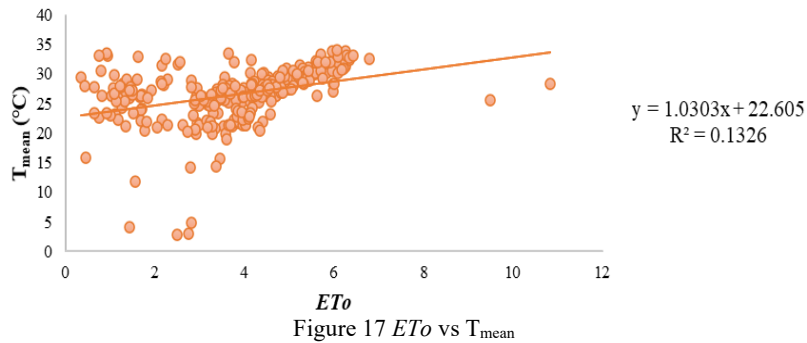
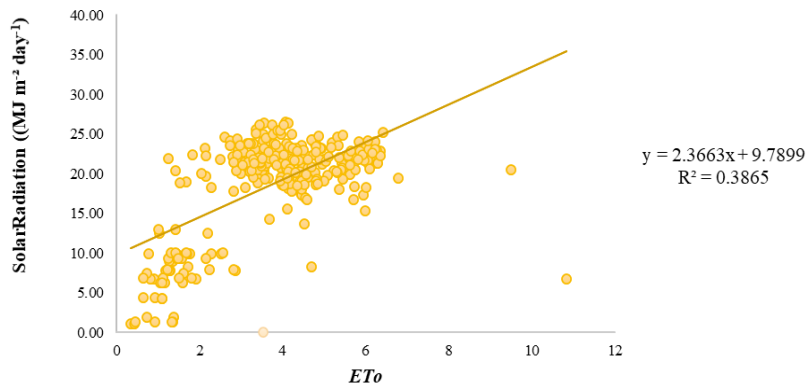
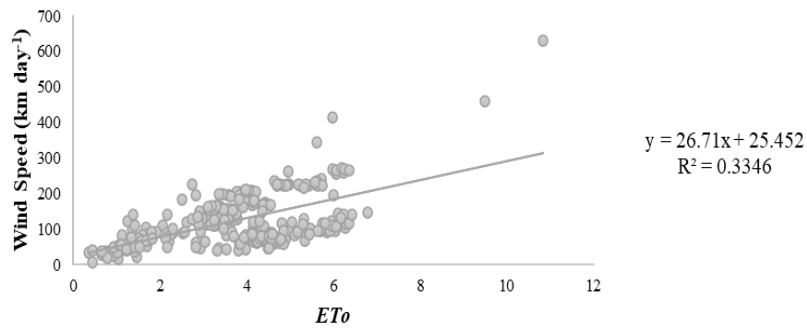


Figure 12 Scatter plot of the GNNTWH input combination

The scatter plot of the various input Combination used for training and validating the FFNN was also developed (not shown). Further analysis was carried out to examine the correlation between each climatological data with Reference *ET* (PM-FAO56). Solar radiation and Wind speed had positive and strong correlation with *ET_o* at a correlation coefficient of 0.621691 and 0.578485 respectively. Mean Temperature had a weak correlation coefficient of 0.33136 and relative humidity had a weak and negative correlation with *ET_o*. Wind speed and solar radiation had a strong correlation with *ET_o* also under the linear regression analysis, this further agrees with the Neural Network solution that wind speed and solar radiation are strong lone inputs in *ET_o* estimation for the Sahel region of Nigeria. The results of the analysis is shown in Figures 15-18. The GRNN is computationally expensive due to its huge size and it has no chance for improvement from optimal methods while the Feed forward neural networks process signals in a one-way direction and have no inherent temporal dynamics. Thus, they are often described as being

static. However, the advantages of FFBP outweighs GRNN in the course of this research.



4 Conclusion

The average runtime for each training and output is 5

seconds, using a system capacity of Intel core (i5) at 2.50 Ghz. 70% of the R values were above 0.5, the optimized spread for all variable combinations varied between 0.23

and 0.95. GRNN combinations of temperature and wind speed (GRNNTW) had the highest statistical indicator for the computation, with $R = 0.7925$, $R^2 = 0.6281$, $MSE = 0.6048$, $RMSE = 0.7777$. GRNNSr (solar radiation alone) had the lowest statistical indicators with $R = 0.3603$, $R^2 = 0.1298$, $MSE = 1.4356$, $RMSE = 1.982$. The lone input of wind speed (GRNNW) compared to the GRNNT, fared better with $R = 0.6457$, $R^2 = 0.4170$, $MSE = 1.0499$, $RMSE = 1.0246$. It can be deduced that wind speed is a much stronger determinant of ET_o than temperature and solar radiation in Kano state, with temperature and solar radiation having $R = 0.4169$, $R^2 = 0.1738$, $MSE = 1.3505$, $RMSE = 1.11623$ and $R = 0.3603$, $R^2 = 0.1298$, $MSE = 1.4356$, $RMSE = 1.1982$ respectively. The input combination of temperature and wind speed is very suitable when using GRNN for obtaining the ET rate in Kano state. The input combination of temperature, wind speed and solar radiation, had the best performance under the FFBBP NN with $R = 0.9111$, $R^2 = 0.8301$, $MSE = 0.4011$, $RMSE = 0.6333$, followed closely by all input combinations of temperature, wind speed, humidity and solar radiation with $R = 0.9090$, $R^2 = 0.8263$, $MSE = 0.3303$, $RMSE = 0.6509$. The temperature and wind speed input combination which ranked first during the GRNN training came third under the FFBBP NN, yet with a better performance than the GRNN, having a performance of $R = 0.8585$, $R^2 = 0.7370$, $MSE = 0.4715$, $RMSE = 0.6866$. It therefore proves the superiority of the FFBBP in predicting ET_o than GRNN for the research area. The lone input of wind speed thrived best under the FFBBP also as a single predictor of ET_o in Kano State with $R = 0.7111$, $R^2 = 0.5056$, $MSE = 0.8446$, $RMSE = 0.9190$. This further shows that wind speed is a better determinant of ET_o in Kano state. Generally, the feedforward backpropagation performed better than the GRNN and agreed fairly with the GRNN in the inputs performance ranking. This has also been reported by several researchers. The work discussed in Salima and Chavula (2012) considered wind speed forecasting by using FFBBP and observed that FFBBP is the best

model. Assi et al. (2013) applied FFBBP for temperature forecasting and concluded that this model had the proper potential for complex modelling of the relation between various factors. Ahmed (2015) stated that FFBBP is one of the most popular configurations of an ANN in his work where he made comparisons between Empirical Models and ANN Method for Global solar radiation at Qena, Egypt. Overall, this investigation shows the superiority of ANN in estimating ET in Kano, part of the Sahelian region of Nigeria over most other empirical formulae indicated.

References

- Ahmed, E. A. 2015. Statistical comparison between empirical models and artificial neural network method for global solar radiation at Qena, Egypt. *Journal of Multidisciplinary Engineering Science and Technology*, 2(7): 1899-1906.
- Antonopoulos, V. Z., and A. V. Antonopoulos. 2017. Daily reference evapotranspiration estimates by artificial neural networks technique and empirical equations using limited input climate variables. *Computers and Electronics in Agriculture*, 132: 86-96.
- Assi, A. H., M. H. Al-Shamisi, H. A. Hejase, and A. Haddad. 2013. Prediction of global solar radiation in UAE using artificial neural networks. In *2013 International Conf. on Renewable Energy Research and Applications (ICRERA)*, 196-200. Madrid, Spain, 20-23 October.
- Deo, R. C., and M. Şahin. 2015. Application of the Artificial Neural Network model for prediction of monthly Standardized Precipitation and Evapotranspiration Index using hydrometeorological parameters and climate indices in eastern Australia. *Atmospheric Research*, 161-162: 65-81.
- FAO. 2011. The state of the world's land and water resources for food and agriculture managing systems at risk. Rome: FAO.
- Feng, Y., Y. Peng, N. Cui, D. Gong, and K. Zhang. 2017. Modeling reference evapotranspiration using extreme learning machine and generalized regression neural network only with temperature data. *Computers and Electronics in Agriculture*, 136: 71-78.
- Gbode, I. E., Akinsanola, A. A, and Ajayi V. O. (2015). Recent changes of some observed climate extreme events in Kano.

- International Journal of Atmospheric Sciences. <http://dx.doi.org/10.1155/2015/298046>.
- Güven, A., and O. Kisi. 2013. Monthly pan evaporation modeling using linear genetic programming. *Journal of Hydrology*, 503: 178-185.
- Hannan, S. A., R. R. Manza, and R. J. Ramteke. 2010. Generalized regression neural network and radial basis function for heart disease diagnosis. *International Journal of Computer Applications*, 7(13): 7-13.
- Heddad, S., Ladlani, I., Houichi, L. and Djemili, L., Modelling Monthly Potential Evapotranspiration (ETP) Using Generalized Regression Neural Networks (GRNN): Case Study of the Semi-Arid Region of GuelmaNortheast of Algeria. *1st International Conference Hydrogeology and Environment SIHE. University Kasdi Merbah - Ouargla 5-7: Novembre 2013-- Ouargla*
- Hosseini, S. M., and N. Mahjour. 2016. Integrating support vector regression and a geomorphologic artificial neural network for daily rainfall-runoff modeling. *Applied Soft Computing*, 38: 329-345.
- Ilesanmi, O. A., P. G. Oguntunde, and A. A. Olufayo. 2014. Evaluation of four ETo models for IITA Stations in Ibadan, Onne and Kano, Nigeria. *Journal of Environment and Earth Science*, 4(5): 89-97.
- Kiş, Ö. 2006. Generalized regression neural networks for evapotranspiration modelling. *Hydrological Sciences Journal*, 51(6): 1092-1105.
- Kriesel, D. 2007. A brief introduction to Neural Networks. Retrieved from <http://www.dkriesel.com>.
- Landeras, G., A. Ortiz-Barredo, and J. J. López. 2008. Comparison of artificial neural network models and empirical and semi-empirical equations for daily reference evapotranspiration estimation in the Basque Country (Northern Spain). *Agricultural Water Management*, 95(5): 553-565.
- Michael, A. M. 1978. Irrigation, theory and practice. Vani Educational Books, India
- Maina, M. M., M. S. M. Amin, W. Aimrun, and T. S. Asha. 2012. Evaluation of different ETo calculation methods: A case study in Kano State, Nigeria. *Philippine Agricultural Scientist*, 95(4): 394-395.
- Nourani, V. 2016. An Emotional ANN (EANN) approach to modeling rainfall-runoff process. *Journal of Hydrology*, 544: 267-277.
- Nwagbara, M. O. 2015. Case study: Emerging advantages of climate change for agriculture in Kano State, north-western Nigeria. *American Journal of Climate Change*, 4(3): 263-268.
- Prasad, R., R. C. Deo, Y. Li, and T. Maraseni. 2017. Input selection and performance optimization of ANN-based streamflow forecasts in the drought-prone Murray Darling Basin region using IIS and MODWT algorithm. *Atmospheric Research*, 197: 42-63.
- Salima, G., and G. M. Chavula. 2012. Determining Angstrom constants for estimating solar radiation in Malawi. *International Journal of Geosciences*, 3(2): 391-397.
- Sengupta, P., J. S. Kinnebrew, S. Basu, G. Biswas, and D. Clark. 2013. Integrating computational thinking with K-12 science education using agent-based computation: A theoretical framework. *Education and Information Technologies*, 18(2): 351-380.
- Singh, P., and M. C. Deo. 2006. Suitability of different neural networks in daily flow forecasting. *Applied Soft Computing*, 7(3): 968-978.
- Specht, D. F. 1991. A general regression neural network. *IEEE Transactions on Neural Networks*, 2(6): 568-576.
- Traore, S., Y. Wang, and T. Kerh. 2008. Modeling reference evapotranspiration by generalized regression neural network in semiarid zone of Africa. *WSEAS Transactions on Information Science and Applications*, 5(6): 991-1000.
- Tuan Resdi, T. A., and W. K. Lee. 2014. Neural Network Hydrological Modeling for Kemaman Catchment. In *Proc. of the International Civil and Infrastructure Engineering Conference 2014*, eds. R. Hassan, M. Yusoff, A. Alisibramulisi, N. Mohd Amin and Z. Ismail, 359-371. Singapore: Springer.
- Ward, A.D., and S.W. Trimble. 2003. *Environmental hydrology*. Boca Raton, FL: Crc Press.